Journal of Geomine (2024), 2(2), 102-120
DOI: 10.22077/jgm.2025.8170.1035

Application of SAM and MTMF methods in differentiating hydrothermal alterations related to metallic mineralization potential, Nignan Exploration Area

Hassan Hosseinzadeh[1], Gholamreza Nowrouzi[2]

Recived: 2024 Sep. 29, Revised: 2025 Apr. 09, Online Published: 2025 Apr. 19

ABSTRACT

Remote sensing data, owing to their extensive spatial coverage, spectral diversity, and integration capabilities, are widely recognized as one of the most effective tools for mineral prospecting. Given that many large mineral deposits are associated with altered zones, identifying these alterations can serve as a valuable guide for mineral exploration. In this study, satellite imagery from ASTER and Sentinel-2A was utilized to detect dolomitic, silicic, iron oxide, sericite, and argillic alterations. To minimize atmospheric effects, radiometric corrections were applied to the data. Subsequently, spectral analyses were conducted using advanced techniques such as the Spectral Angle Mapper (SAM), Matched Filter (MF), and Mixture Tuned Matched Filter (MTMF) methods. These approaches were employed to enhance the accuracy of alteration mapping. The results obtained from these methods were consistent with those derived from band ratio techniques and false-color composite imagery, further validating the findings. The northern and southern regions of the study area were identified as highly promising zones for mineralization. A strong correlation was observed between the identified alterations and geological lineaments, indicating significant mineral potential in these areas. To further refine the assessment of this potential, it is recommended that future studies integrate ground-based surveys and geochemical analyses. Such complementary approaches would provide a more comprehensive understanding of the mineralization processes and improve the precision of resource estimation.

KEYWORDS

Cement, Gypsum, Limestone, Manufacturing, Petrography

I. INTRODUCTION

Remote sensing is the science of acquiring information about objects by measuring electromagnetic radiation, primarily through the reflection and emission of sunlight, without direct physical contact. This data, when properly processed and analyzed, can provide valuable insights about the studied area(Aggarwal, 2004; Campbell et al., 2011; Schowengerdt, 2006). Nowadays, remote sensing techniques are widely utilized in various fields, one of the most significant applications being mineral resource exploration. Remote sensing allows for the accurate and rapid identification of mineral deposits across large areas, both directly and indirectly, at low costs. It is also widely used in preliminary exploration to produce geological base maps and to identify and differentiate mineralization-controlling features (Amer et al., 2012; Pour et al., 2013; Sadek et al., 2006; Shebl et al., 2021). Satellite data are collected digitally, allowing for the application of mathematical methods and image processing techniques to enhance and clarify the data. Remote sensing is especially valuable for detecting lineaments and identifying altered zones, key indicators in geological studies. Lineaments, which include faults, joints, and fractures, can serve as pathways for mineral-rich fluids and help pinpoint potential mineralized zones. Remote sensing techniques such as directional filtering and edge detection analysis are instrumental in detecting these geological structures, which play a critical role in locating mineral deposits (Ahmadi et al., 2021; Dasgupta et al., 2019; Marghany et al., 2010).

Hydrothermal alterations, resulting from chemical changes in rocks due to hot fluids, are often associated with significant mineral deposits. Spectral data obtained from remote sensing can detect the spectral differences between various minerals, accurately identifying altered zones that often indicate the presence of valuable metals such as copper and gold (Hdeid et al., 2024; Pour et al., 2013; Yao et al., 2021).

ASTER and Sentinel-2A satellite imagery are commonly used in geological studies and mineral

[1] Master of mining engineering, Department of Mining Engineering, Faculty of Engineering, University of Birjand, Birjand, Iran, [2] Department of Mining Engineering, Faculty of Engineering, University of Birjand, Birjand, Iran
✉ H. Hosseinzadeh: Hosseinzadeh.hassan70@gmail.com

exploration to identify alterations and lineaments. Each of these satellites offers unique spectral features that are particularly effective in highlighting geological structures and hydrothermal alteration minerals. ASTER imagery, with its shortwave infrared (SWIR) and thermal bands, is highly effective in identifying minerals associated with argillic and phyllic alterations, allowing for detecting areas with mineralization potential. Additionally, Sentinel-2A imagery, with its high spectral resolution, allows for the detailed identification of lineaments and fractures (Chen et al., 2022; Hu et al., 2018; Tompolidi et al., 2020).

Directional filters, a type of image processing method in remote sensing, are used to detect abrupt changes in reflectance in various directions, helping to identify lineaments such as geological faults and fractures. These methods enhance linear structures, providing useful information about potential pathways for mineral fluid flow and thus potential mineralized areas (Ahmadi et al., 2021).

Techniques for highlighting hydrothermal alterations, including false-color composites, band ratios, SAM (Spectral Angle Mapper), and MTMF (Matched Filter and Mixture Tune Matched Filter), are powerful tools for identifying hydrothermal alteration minerals on the surface. False-color composites visually display spectral differences between rocks and minerals by combining appropriate bands. In contrast band ratios enhance specific spectral features of alteration minerals, such as iron-rich or clay minerals. The SAM method identifies alteration zones by comparing the spectral signature of each pixel to that of target minerals. The MTMF method, a specialized tool for processing hyperspectral data, operates in two stages. First, the Matched Filter (MF) directly detects pixels similar to the target spectrum, generating a probability map for the presence of the desired mineral or feature. In the second stage, MTMF uses noise and background information to separate the pixels related to the target mineral from the background, increasing detection accuracy. This technique, by reducing noise and focusing on specific spectral features, is effectively employed in identifying potential mineralized areas (Honarmand et al., 2018; Hosseinjani et al., 2011; Yousefi et al., 2018). The primary objective of this study is the delineation and identification of hydrothermal alteration zones associated with lead-zinc mineralization in the Neygan exploration area, utilizing satellite imagery and advanced image processing techniques. This research focuses on the analysis of remote sensing data and the application of sophisticated image processing methods to detect spectral patterns linked to alteration minerals such as sericite, chlorite, carbonates, iron oxides, and silica. These minerals are key indicators for identifying hydrothermal environments and base metal mineralization. The outcomes of this study are anticipated to reduce exploration costs and time while providing enhanced insights into the controlling mechanisms of mineralization and the evolutionary processes of hydrothermal systems within the Nignan region.

II. Literature Review

In remote sensing studies and mineral exploration, various methods have been employed to identify and highlight alterations associated with mineral deposits. Among these, false-color composites and band ratios are considered fundamental and initial techniques. Due to their simplicity and quick application, they play a significant role in the early stages of satellite image processing. These methods visually differentiate spectral variations between rocks and minerals by combining different bands from multispectral images. For example, by selecting three specific bands from satellite images and assigning them to the red, green, and blue channels, areas with potential alterations can be highlighted. Moreover, band ratios create a ratio between specific bands, which is particularly effective in identifying iron-bearing and clay minerals, enhancing the visibility of alteration zones. However, despite their usefulness in distinguishing initial spectral variations, these methods have limitations. Due to spectral interferences and noise in the data, false-color composites and band ratios may face challenges in accurately identifying specific minerals and differentiating alteration zones. Therefore, advanced methods such as SAM have become necessary. SAM compares the spectral signature of each pixel with the spectral signature of target minerals, identifying regions with similar spectral characteristics. One of the main advantages of SAM is that it reduces the impact of lighting variations, making it especially effective for accurately identifying alteration minerals across different areas. This method is highly efficient in delineating mineral potential zones and can be considered a more advanced tool than basic false-color composites and band ratios. However, SAM also has limitations when detecting regions with low signal-to-noise ratios. This is where the MTMF method emerges as a more powerful tool. MTMF combines spectral matching techniques with noise reduction, allowing not only the identification of pixels with spectra close to the target but also the removal of noise and background information from the results. Consequently, identifying minerals and alterations is carried out with higher accuracy. In summary, false-color composites and band ratios are helpful for quickly and initially identifying alteration zones. However, due to limitations in accurately distinguishing minerals, more advanced methods such as SAM and MTMF become essential. SAM focuses on precise spectral comparison, while MTMF excels in noise reduction and highlighting specific features, making them highly efficient tools for detailed

mineral exploration and identifying areas with high mineral potential (Amer et al., 2012; Hosseinjani et al., 2011; Kodama et al., 2010; Yousefi et al., 2018).

One of the early studies in this field was conducted by van der Meer et al. (2012), which assessed the effectiveness of various image-processing methods for identifying and mapping mineral alterations. The study concluded that spectral methods such as SAM and MTMF, particularly when combined with hyperspectral data, are highly accurate in identifying minerals associated with mineral deposits. The research highlighted that MTMF performs better under complex spectral conditions, providing detailed insights into target areas, and underlining its importance in mineral exploration (Van der Meer et al., 2012). Additionally, Pour and Hashim (2014) utilized the MTMF method on hyperspectral Hyperion data in southern Iran, demonstrating that this method is exact and effective in identifying and distinguishing minerals associated with hydrothermal gold deposits. Their findings showed that MTMF, by eliminating noise and irrelevant information, has a high capability in highlighting target minerals and determining areas with mineral potential (Beiranvand Pour et al., 2014). Honarmand et al. (2018) examined the effect of using different reference spectra in the SAM method for mapping hydrothermal alterations in the Cenozoic Magmatic Arc of Kerman (KCMA), Iran. This area includes significant porphyry copper deposits such as the Miduk and Chah-Firouzeh mines. In this study, three types of reference spectra, including image spectra, USGS spectral library, and field samples, were used for the SAM algorithm. The results were evaluated and confirmed by field investigations and laboratory analyses, including thin section studies, XRD analysis, and VNIR-SWIR reflectance spectroscopy. The highest accuracy of 74.01% and a Kappa coefficient of 0.65 were achieved using field sample spectra as the reference. SAM results were also compared with the MTMF method, revealing that over 90% of the known copper mineralization zones were within the enhanced alteration zones (Honarmand et al., 2018). Nouri et al. (2019) focused on using ASTER sensor data to identify hydrothermal alteration zones related to polymetallic mineralization in the Toroud-Chah Shirin magmatic belt in northern Iran. The researchers employed techniques such as Selective Principal Component Analysis (SPCA), Band Ratio Matrix Transformation (BRMT), SAM, and MTMF. The results effectively identified alteration zones and mineral assemblages, which were validated through fieldwork and laboratory analyses (Noori et al., 2019). Similarly, Esmaeilzadeh et al. (2023) identified hydrothermal alterations associated with porphyry copper-gold mineralization in the Sonajil region of Iran using ASTER data and various image processing techniques. Spectral methods such as SAM and MTMF were applied for precise alteration detection. SAM helped identify specific minerals based on reference spectra, while MTMF distinguished the target mineral spectra from complex backgrounds. The results showed a strong correlation with regional lithology, confirming the presence of porphyry deposits, and further geochemical and geophysical investigations were recommended (Esmaeilzadeh et al., 2023).

Overall, these credible studies demonstrate that SAM and MTMF methods are advanced and practical tools for identifying and mapping mineral alterations. Utilizing these methods significantly enhances the accuracy and efficiency of exploratory studies.

III. Geology of the Study Area

The study area is part of east of Iran and located 50 km northwest of Boshrouyeh, in the Ferdows County, and 16 km west of the village of Nignan. It is part of the 1:100,000 geological map of Eshqh Abad (Aghanabati et al., 1994) (**Error! Reference source not found.**). According to the map, the Yaghman Shah rock formation consists of pink to yellow marls, dark gray shales, and sandstone with interbeds of sandy limestones. Overlying the Yaghman Shah formation is a sequence of limestone, marl, and shale belonging to the Ghal'eh Dokhtar formation. Most of the lead and zinc mineral deposits and indications in this area are associated with the dolomitic and limestone formations of Shotori, Jamal, and Shemshak. These deposits are often related to faults within the limestone-dolomitic formations (Aghanabati et al., 1994).

IV. Preprocessing and Processing of Satellite Images

A. Satellite Images

The ASTER sensor is a multispectral sensor developed by NASA and METI (Japan's Ministry of Economy, Trade, and Industry). This sensor covers three spectral ranges: Visible and Near Infrared (VNIR) bands, ranging from 0.52 to 0.86 μm; Shortwave Infrared (SWIR) bands, ranging from 1.6 to 2.43 μm; and Thermal Infrared (TIR) bands, ranging from 8.125 to 11.65 μm. These capabilities allow ASTER to provide valuable information regarding surface characteristics, including mineral compositions and thermal variations (Schmugge et al., 2003). Sentinel-2, part of the European Union's Copernicus program, is managed by ESA (European Space Agency). This multispectral sensor contains 13 bands, including VNIR bands from 0.4 to 1.0 μm and SWIR bands ranging from 1.375 to 2.28 μm. Sentinel-2 also includes special bands for water detection and vegetation monitoring (Spoto et al., 2012).

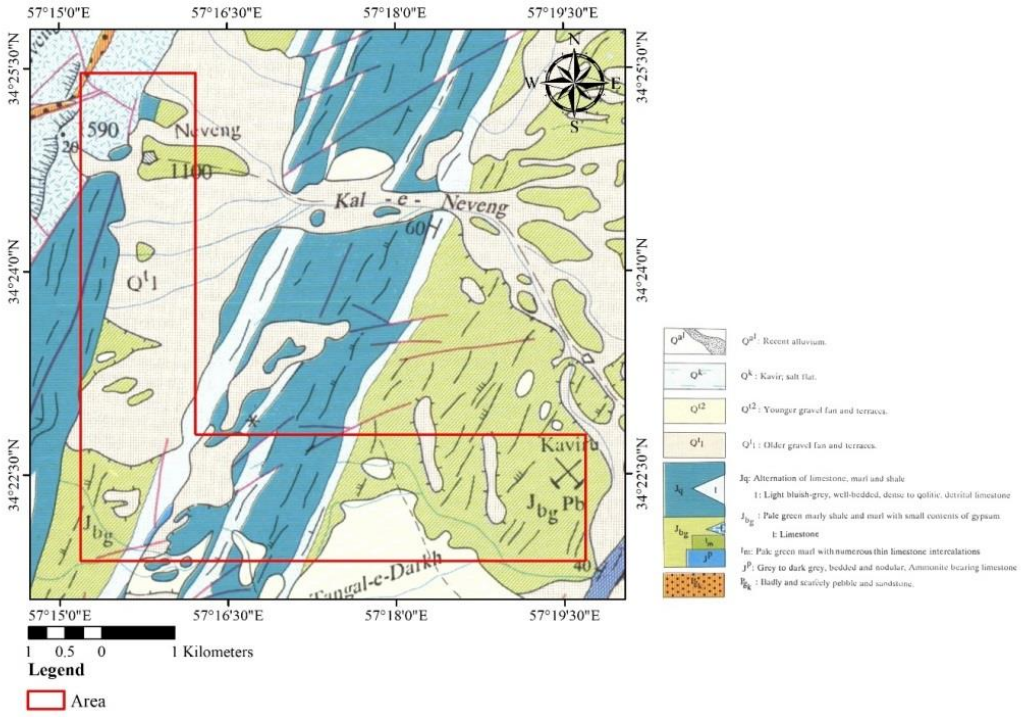

Fig. 1. Geological Map of the study area based on the 1:100,000 geological map of ESGH ABAD

The SWIR bands on the ASTER sensor (bands 5 to 9) are crucial for detecting clay and silicate minerals such as kaolinite, montmorillonite, illite, and sericite found in argillic and phyllic alterations, as well as chlorite, epidote, and sericite in propylitic alteration zones. These minerals exhibit distinctive reflective characteristics in the SWIR bands. Specifically, clay minerals and phyllosilicates are well-recognized in these bands due to their strong reflection and distinctive absorption features in this spectral range. Additionally, the TIR bands (bands 10 to 14) on ASTER are particularly effective for identifying silicate minerals such as quartz and feldspar, commonly present in phyllic alteration zones and silicification. Quartz, often found in alteration zones associated with metal deposits, exhibits strong reflectance in thermal bands, making it easily identifiable. Thermal and hydrothermal alterations, often accompanied by temperature shifts and silicification, can also be detected using TIR bands. Sentinel-2 features numerous bands within the VNIR range highly sensitive to iron oxides. These bands reveal strong reflectance from iron oxides like hematite, limonite, and goethite, making it possible to identify these mineral changes due to their distinctive reflectance in this spectral range (Hu et al., 2018; Kabolizadeh et al., 2022) (Fig. **1**).

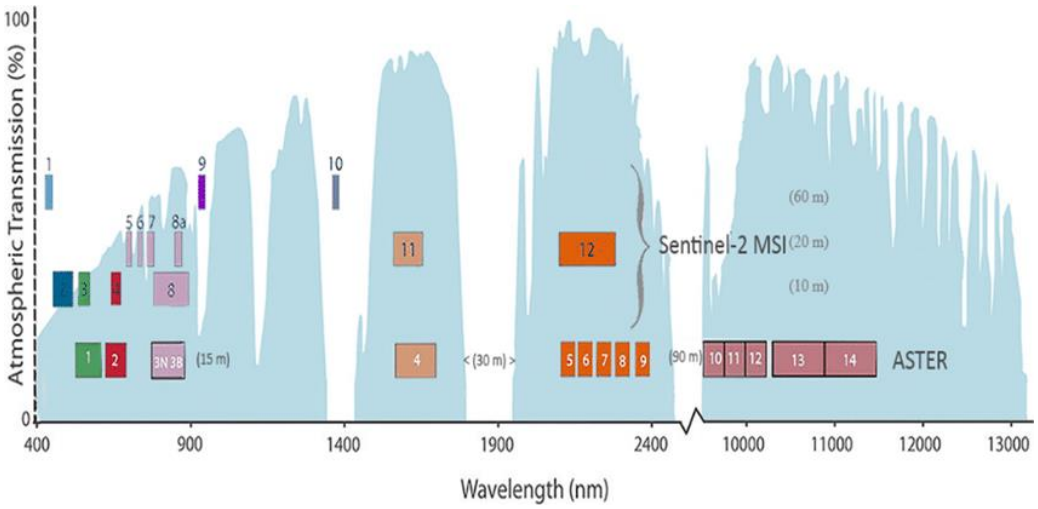

Fig. 1. Comparison of ASTER and SENTINEL Bands (Kabolizadeh et al., 2022)

B. Pre-Processing of Satellite Images

1) Radiometric correction

Radiometric correction refers to a process where the brightness values or pixel intensities of a satellite image are adjusted to eliminate or reduce atmospheric effects, solar angle variations, and surface conditions. These corrections enhance the quality of images, making the data more reliable for quantitative and qualitative analysis in fields like geology, agriculture, and environmental studies. Atmospheric effects such as light absorption and scattering by air molecules and suspended particles can alter the amount of energy reaching the sensor. Additionally, variations in solar illumination angle and topographical conditions like slope and surface orientation can influence reflected light intensity. The Internal Average Relative Reflectance (IARR) method is a straightforward and practical approach for radiometric correction, especially in situations where atmospheric data is unavailable or calibrated images are not accessible. IARR operates on the assumption that each satellite image contains areas with relatively consistent reflectance across the entire image. To implement IARR, the average reflectance of all pixels in each spectral band is calculated. Then, the reflectance of each pixel in each spectral band is divided by the average of that band. This process mitigates external factors such as atmospheric conditions and solar angles, resulting in an image that better reflects surface features without atmospheric interference. One of the key advantages of the IARR method is that it does not require external data or complex atmospheric models, making it highly suitable for areas where precise atmospheric data is unavailable (Bernstein et al., 2012; Kayadibi, 2011). Fig. 3 Shows the Spectral Profile of a Pixel before and after IARR correction.

2) Vegetation Removal

In geological studies, particularly when investigating hydrothermal alterations, removing vegetation and utilizing the Normalized Difference Vegetation Index (NDVI) is crucial. NDVI is a tool for detecting and assessing vegetation cover. Healthy vegetation reflects high near-infrared and low red light, which results in higher NDVI values. Conversely, areas with sparse or no vegetation yield lower NDVI values.

$$NDVI = \frac{NIR - Red}{NIR + Red} \quad (1)$$

In geological surveys, vegetation cover can obscure the underlying geological features. Hydrothermal alterations are often detected by spectral differences in the reflected light from minerals, but vegetation may mask these reflective patterns, making mineral spectral analysis difficult. Removing vegetation from satellite or aerial images allows geologists to focus more on the underlying geological structures and areas with potential alterations (Okada et al., 1993; Pour et al., 2013).

C. Satellite Image Processing

1) Lineament Enhancement using Directional Filters

Directional filters are employed in image processing to detect edges and structural features in specific directions. These filters analyze variations in intensity across different directions, enhancing structures such as lineaments (distinct lines or edges) in satellite images. Directional filters are a spatial filter that is applied to images as small matrices. They use convolution to measure intensity changes across various directions. The filters are tuned to specific orientations (e.g., 0, 45, 90, and 135 degrees), with convolution being a mathematical operation where the filter (or kernel) is applied over the original image. Each filter element is multiplied by the pixel values within a specific image area, and the results are summed. This process highlights particular features and identifies sudden changes in intensity. Lineaments often appear as edges in satellite images, reflecting abrupt shifts in brightness or reflectance, possibly indicating geological structures such as faults, fractures, or lithological boundaries. Directional filters are designed to be sensitive to changes in a specific direction. For instance, 0° and 90° filters detect horizontal and vertical changes, while 45° and 135° detect diagonal changes. When applied to an image, the directional filter calculates brightness variations in the designated direction. Sudden changes, such as a lineament, will be highlighted and clearly shown after filtering. By identifying these sudden brightness variations and enhancing them in various directions, directional filters assist in detecting lineaments in satellite images. These filters make it easier to identify linear structures, such as faults or other geological features, prominently visible in the images (Marghany et al., 2010; Scharcanski et al., 1997; Trahanias et al., 1996).

After enhancing potential lineaments using directional filters in ENVI software, the lineaments were accurately extracted using Geomatica software (Fig. 3 and Fig. 4).

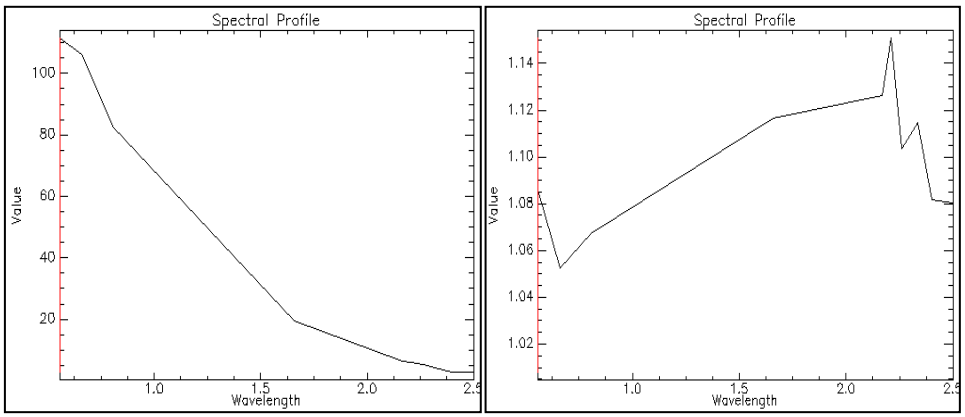

Fig. 2. Spectral Profile of a Pixel before and after IARR correction

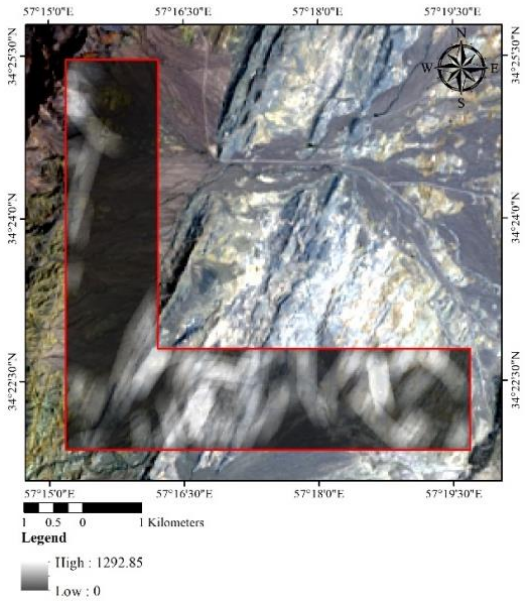

Fig. 3. Density Map of the probable lineaments extracted

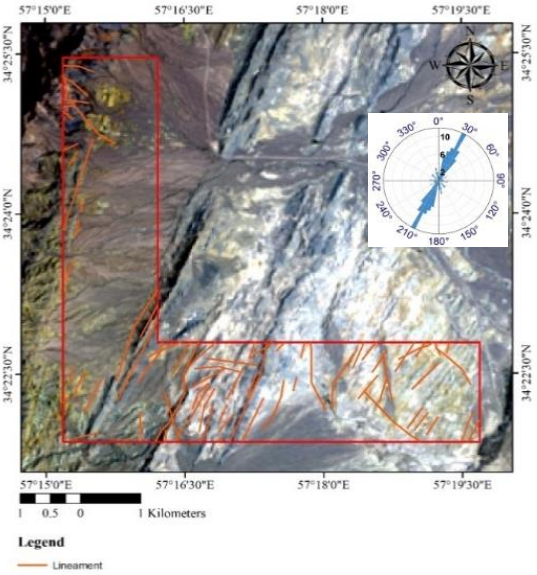

Fig. 4. Probable Lineaments of the Study Area extracted from SENTINEL 2A imagery and the rose diagram of the lineaments

2) False Color Composite

Satellite images, particularly multispectral ones, operate in different spectral ranges and capture images in various bands. There are two primary methods for displaying and analyzing multispectral satellite images: True Color Composite and False Color Composite.

- True Color Composite: In this method, the spectral bands closest to the visible range of human sight (red, green, and blue) are assigned to the red (R), green (G), and blue (B) channels of the image, respectively. This combination creates an image resembling how the human eye would naturally views the landscape. It accurately depicts surface features such as vegetation, water, roads, and buildings.

- False Color Composite: In this technique, spectral bands are selected in a way that doesn't necessarily correspond to human-visible colors. For instance, Near-Infrared (NIR) bands are often assigned to one of the visible color channels (red, green, or blue). This method helps highlight specific features of the Earth's surface that are not readily observable in true-color composite images. False color composite is frequently used for analyzing vegetation, identifying mineral alterations, or studying geological structures.

As a result, true color composite is utilized for a natural representation of the Earth's surface, whereas false color composite is used to emphasize particular features not easily visible in the visible spectral range (Boloki et al., 2010; Feizi et al., 2012).

In this study, the RGB=432 combination from Landsat 8 satellite imagery was used to display the true color composite of the region (Fig. 5).

The false color composite with RGB=468 from ASTER satellite imagery was employed to visualize alteration zones associated with mineralization. In this composite, propylitic alterations are displayed in shades of green to blue, while argillic alterations appear in pink to red. Furthermore, the false color composite with RGB=461 in ASTER images displayed argillic alterations and iron oxides. In this combination, argillic alterations appear green to blue, and iron oxides are visualized in red to orange (Feizi et al., 2012) (Fig. 6 and Fig. 7).

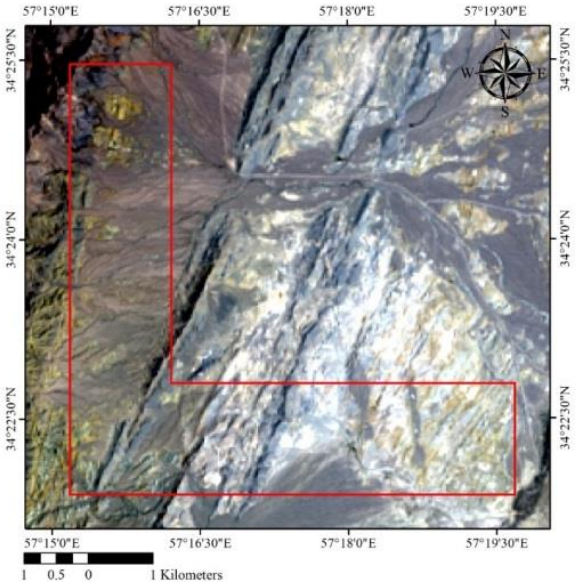

Fig. 5. True Color Composite (RGB432) from Landsat satellite imagery

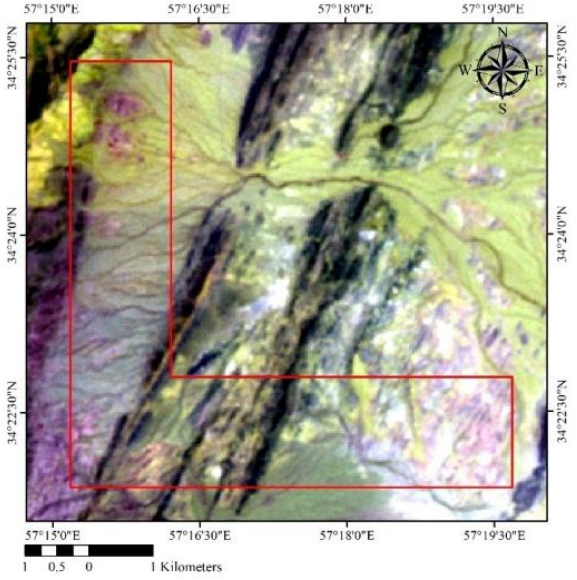

Fig. 6. RGB468 from ASTER satellite for displaying propylitic (olive green) and argillic (pink) alterations

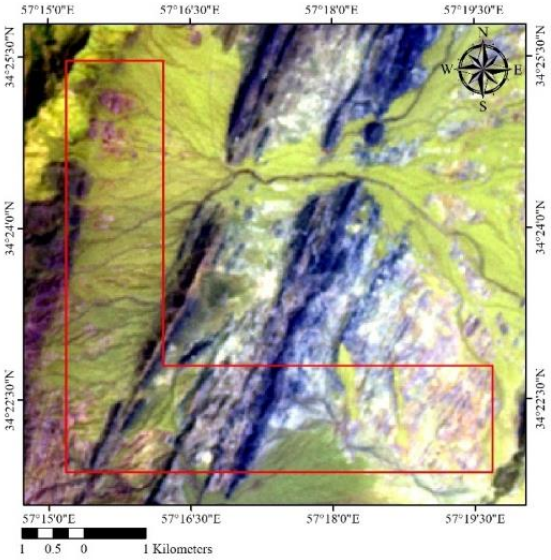

Fig. 7. RGB461 from ASTER satellite to show sericitic and argillic alterations (green to blue) and iron oxides (red to orange)

3) Band Ratio Method

The band ratio method is one of the most widely used techniques for identifying areas containing specific minerals. In this method, to generate an image highlighting a particular mineral or alteration type, the band in which the mineral has the highest reflectance is divided by the band with the highest absorption. The result is a black-and-white image where bright spots indicate the highest ratio values, signifying the greatest likelihood of the target mineral's presence (Kasmaeeyazdi et al., 2022; Pour et al., 2018).

In this study, various band ratios (Table 1) were used to enhance iron oxides, argillic alterations, silicification, dolomitization, and sericitization, all associated with metal mineralization. The results, along with explanations, are provided in Fig. 8 through Fig. 19.

All black-and-white images generated by various methods were classified using the thresholding method based on the mean and standard deviation. For images where high values are favorable, the anomaly threshold was set at $\mu+2\sigma$, and for images where low values are favorable, the anomaly threshold was set at $\mu-2\sigma$.

Table 1:Band ratios used in this research

Satellite image	Bandratio	Description	Reference
ASTER	2/1	Areas containing ferric iron oxide (Fe^{3+})	(Ding et al., 2023)
	(5/3)+(1/2)	Areas containing ferrous iron oxide (Fe^{2+})	
	(7+9)/8	Areas containing carbonates, chlorite, and epidote	
	(6+9)/(7+8)	Areas containing chlorite and epidote	
	(6+8)/7	Areas containing dolomite	
	(5+7)/6	Areas containing muscovite, illite, and smectite	
	(4+6)/5	Identification of areas containing alunite and kaolinite	
	14/12	Identification of areas containing quartz	
SENTINEL 2A	4/2	Areas containing iron oxides	(Kasmaeeyazdi et al., 2022)
	4/3	Areas containing iron oxides	
	11/8	Areas containing ferric iron oxide (Fe^{3+})	
	4/11	Areas containing ferrous iron oxide (Fe^{2+})	

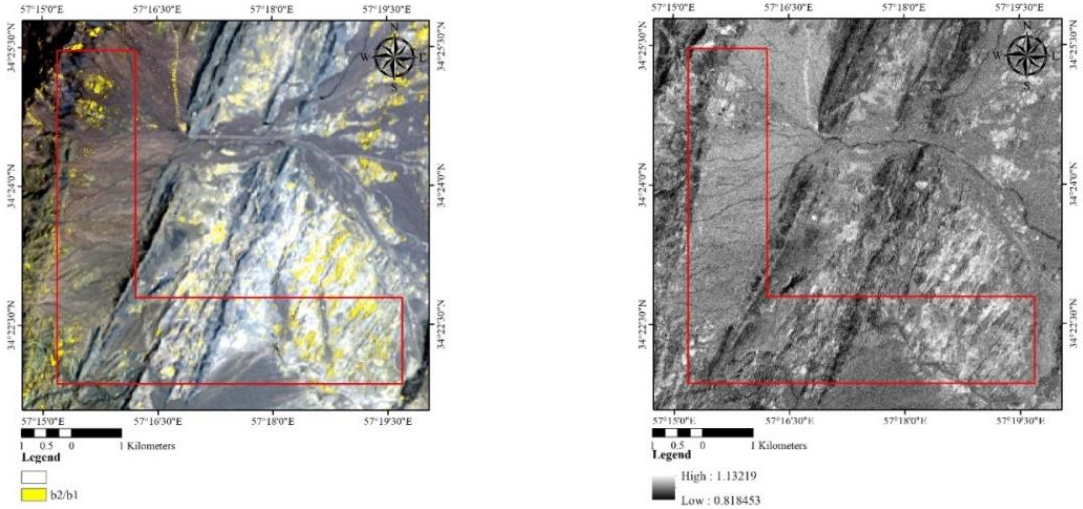

Fig. 8. Band ratio 2/1 of ASTER satellite imagery for the identification of areas containing ferric iron oxide (Fe^{3+})

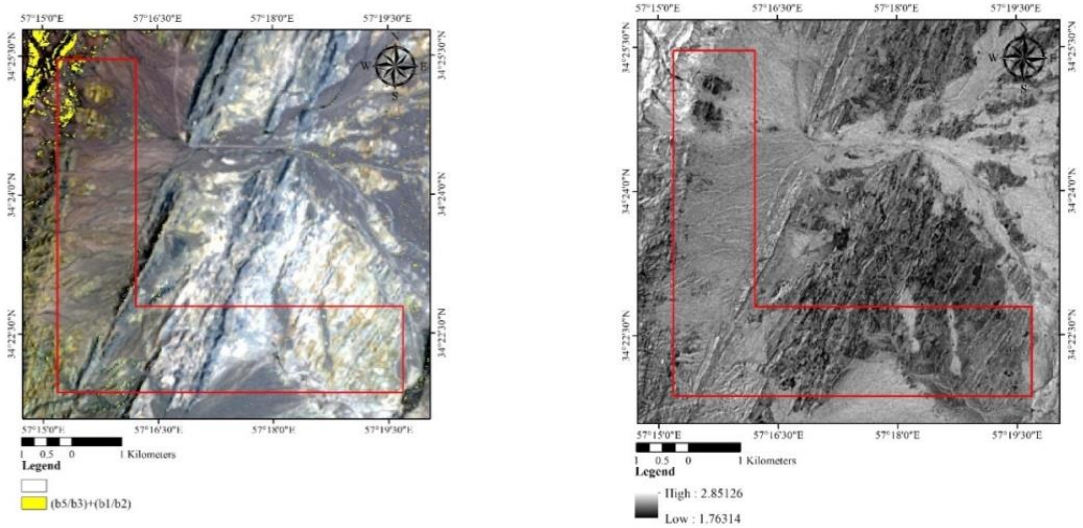

Fig. 9. Band ratio (5/3) + (1/2) of ASTER satellite imagery for the identification of areas containing ferrous iron oxide (Fe^{2+}).

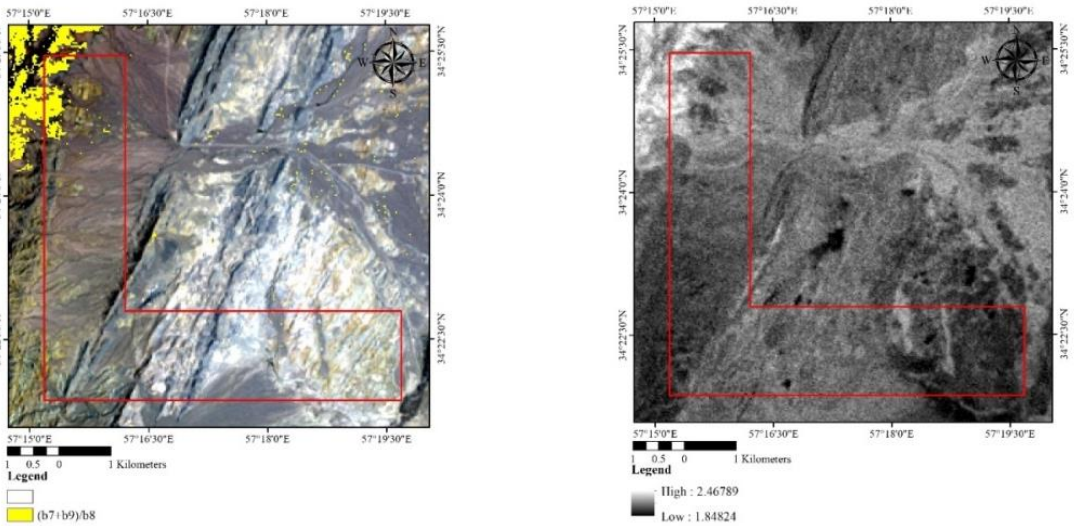

Fig. 10. Band ratio (7+9)/8 of ASTER satellite imagery for the identification of areas containing carbonates, chlorite, and epidote

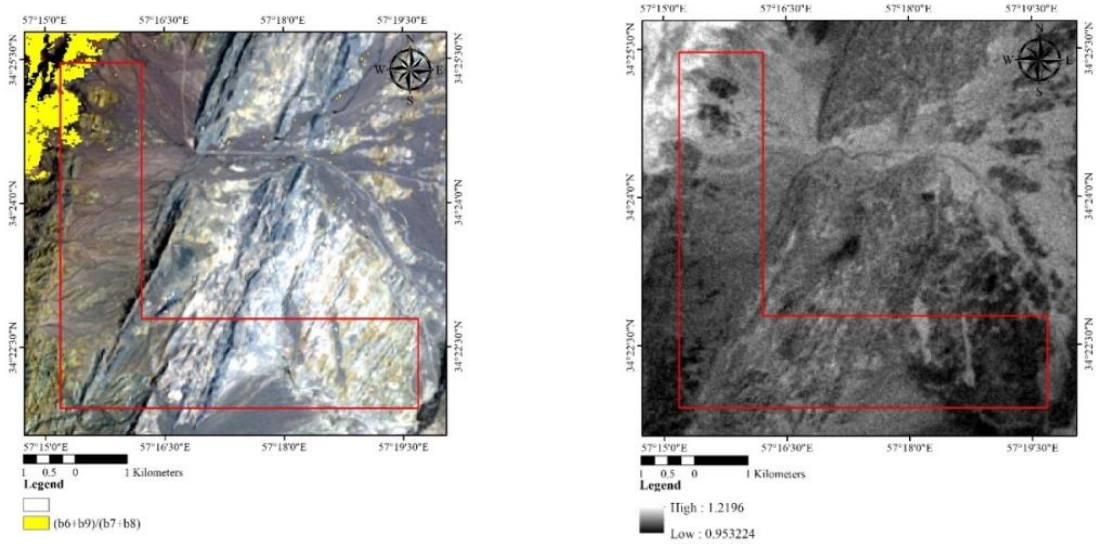

Fig. 11. Band ratio (6+9)/(7+8) of ASTER satellite imagery for the identification of areas containing chlorite and epidote

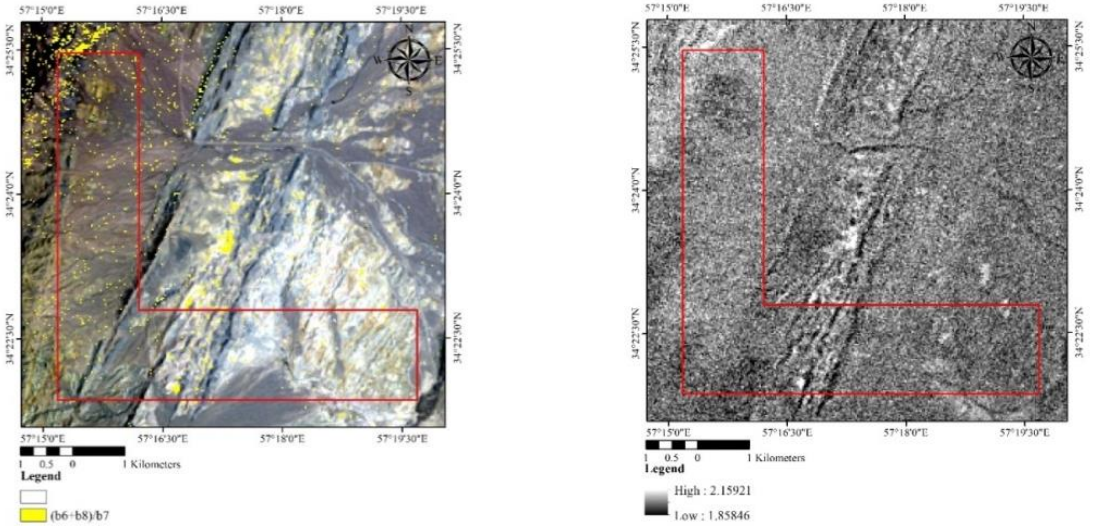

Fig. 12. Band ratio (6+8)/7 of ASTER satellite imagery for the identification of areas containing dolomite

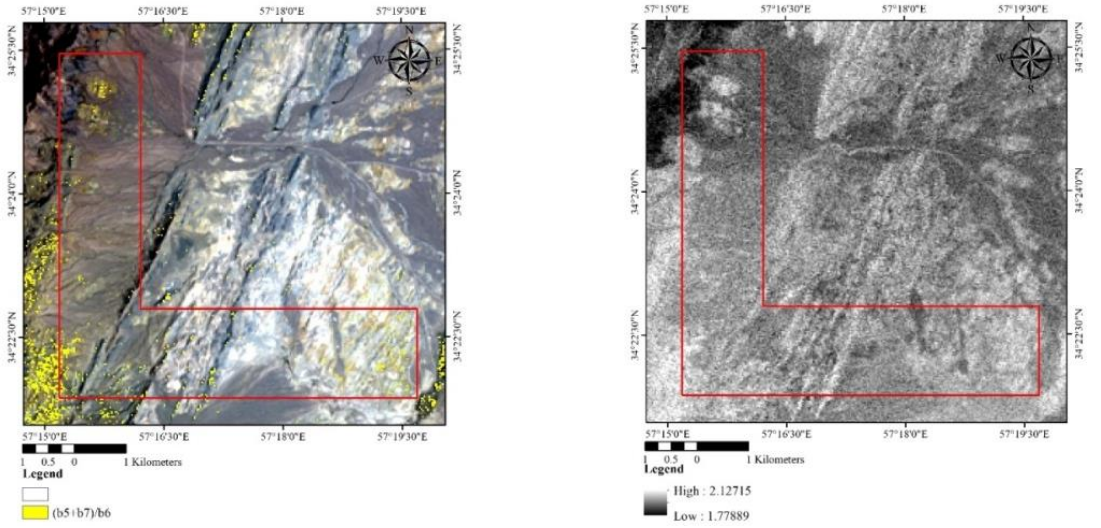

Fig. 13. Band ratio (5+7)/6 of ASTER satellite imagery for the identification of areas containing muscovite, illite, and smectite

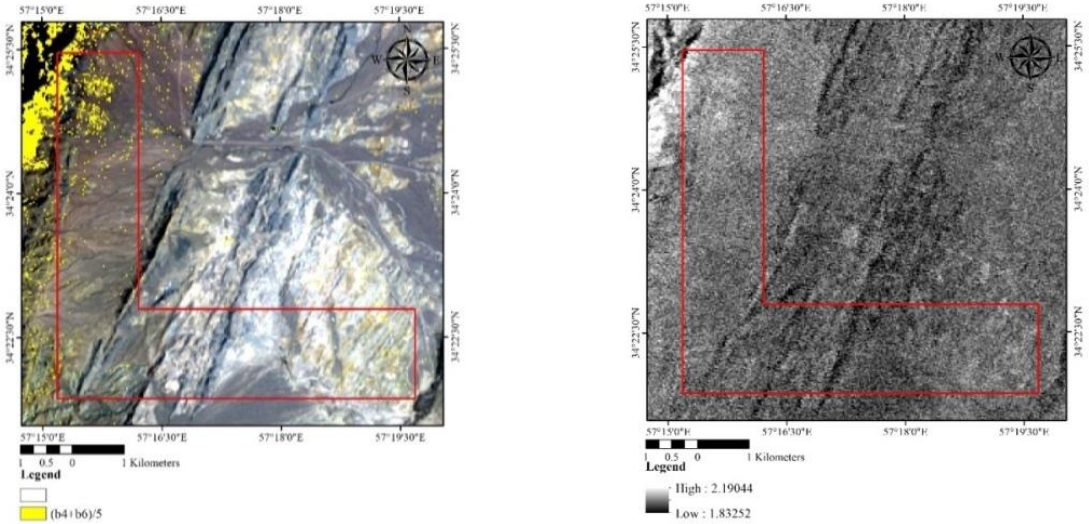

Fig. 14. Band ratio (4+6)/5 of ASTER satellite imagery for the identification of areas containing alunite and kaolinite

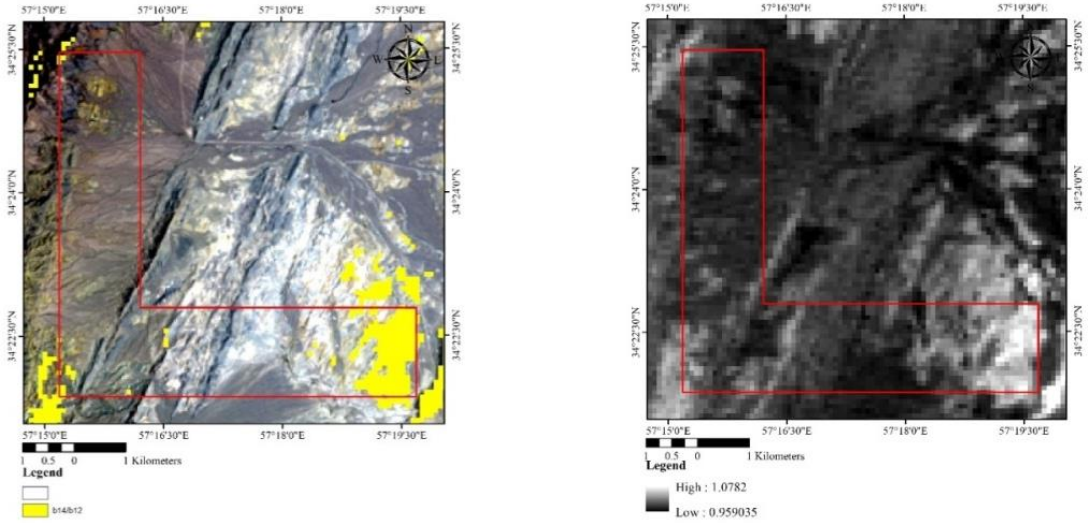

Fig. 15. Band ratio 14/12 of ASTER satellite imagery for the identification of areas containing quartz

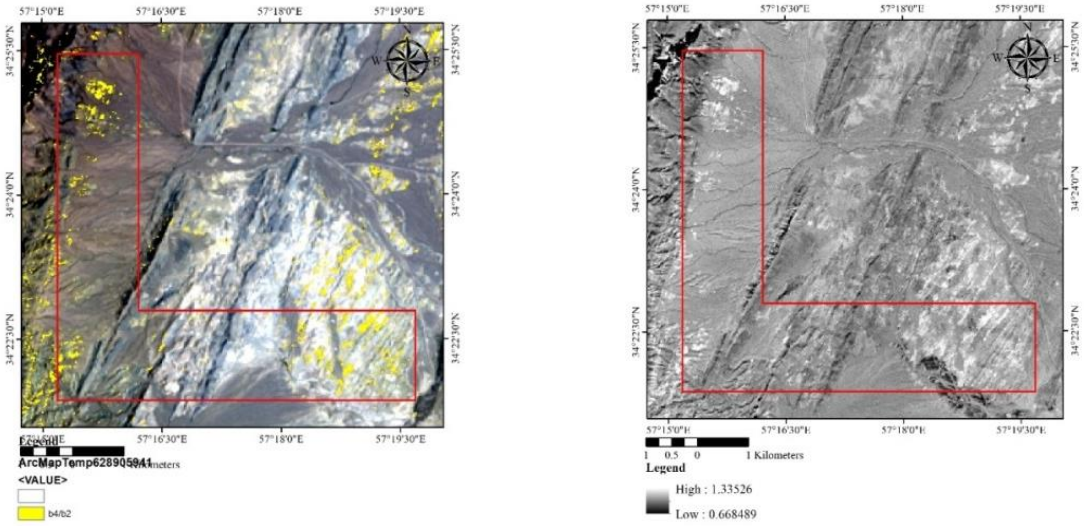

Fig. 16. Band ratio 4/2 of Sentinel satellite imagery for the identification of areas containing iron oxides

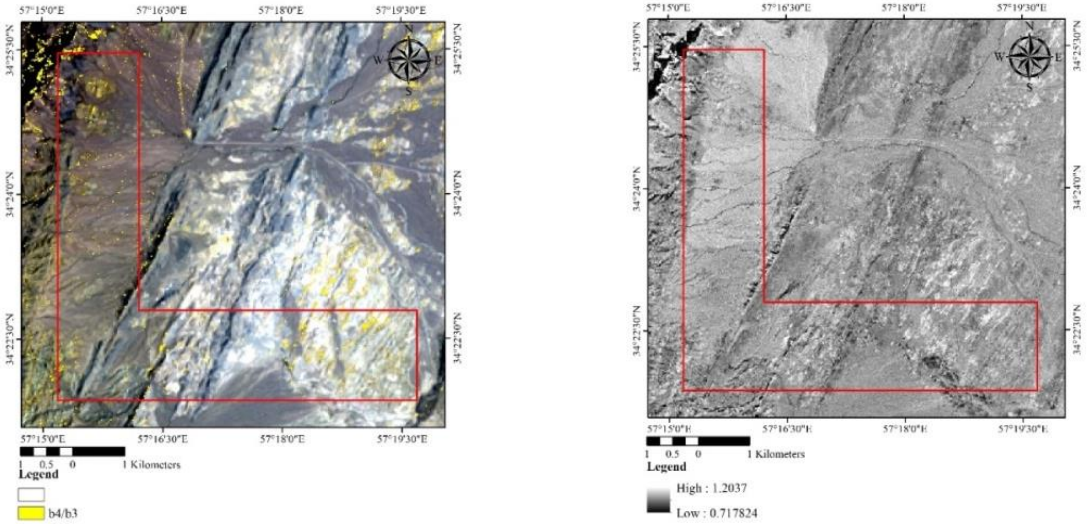

Fig. 17. Band ratio 4/3 of Sentinel satellite imagery for the identification of areas containing iron oxides

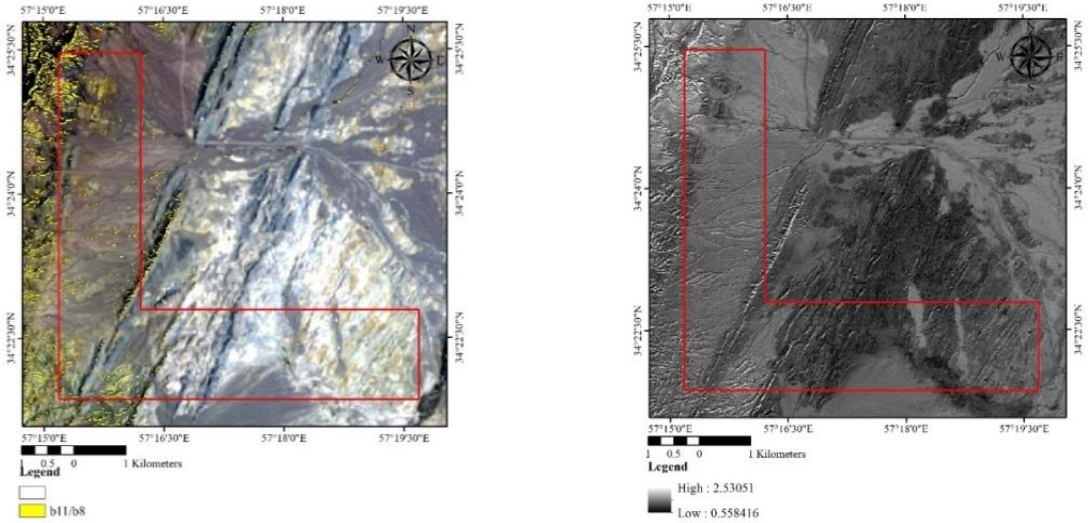

Fig. 18. Band ratio 11/8 of Sentinel satellite imagery for the identification of areas containing ferric iron oxide (Fe^{3+})

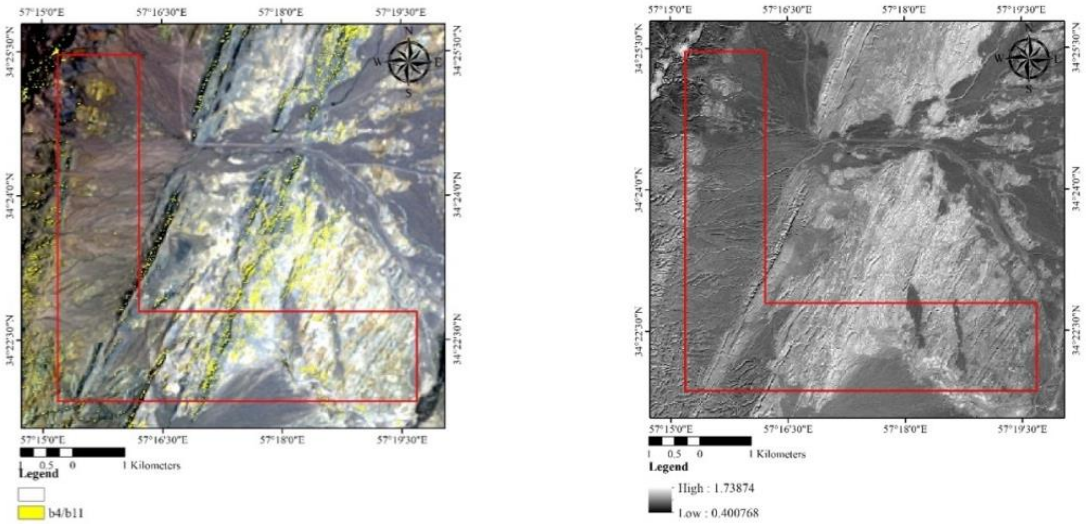

Fig. 19. Band ratio 4/11 of Sentinel satellite imagery for identifying areas containing ferrous iron oxide (Fe^{2+})

D. Advanced ASTER Image Processing

In this section, endmembers (minerals) from ASTER satellite imagery were extracted using the Sequential Maximum Angle Convex Cone (SMACC) algorithm. These endmembers were then compared with spectral libraries to identify mineral types and determine the alteration zones in the study area.

1) Selecting the Appropriate Spectral Profile

An endmember is the reflectance spectrum of a pure material detected by the sensor. Spectra extracted from satellite imagery that represent specific materials are referred to as endmembers. In this study, the SMACC algorithm (Gruninger et al., 2004) was used to extract endmembers from ASTER satellite images of the Shadan region .

After initial corrections, a 6-band set from the imagery was prepared. Given the presence of 6 separate bands in the shortwave infrared (SWIR) range of the electromagnetic spectrum, the ASTER sensor easily differentiates and classifies various minerals in porphyry copper alteration zones. Clay minerals, due to the presence of AlOH and MgOH bonds in their composition, exhibit high absorption at wavelengths of 2.22 µm, 2.17 µm, 2.26 µm, and 2.35 µm, which enables their better identification (Hosseinjani et al., 2011).

In this research, 30 endmembers were extracted from the 6-band set. These were compared to 6-band spectra from the USGS spectral library, and the endmembers that closely matched alteration-related minerals associated with porphyry copper deposits were selected.

2) Identifying and Selecting Extracted Endmembers

From the 30 extracted endmembers, after comparison with reference spectra, key endmembers related to alteration minerals were identified. Endmembers 8 and 17 were selected for dolomite and calcite, 20 and 29 for chlorite and epidote, 13 and 18 for jarosite, 28 for kaolinite, and 7, 12, 14, and 22 for muscovite (Fig. 20 to Fig. 24).

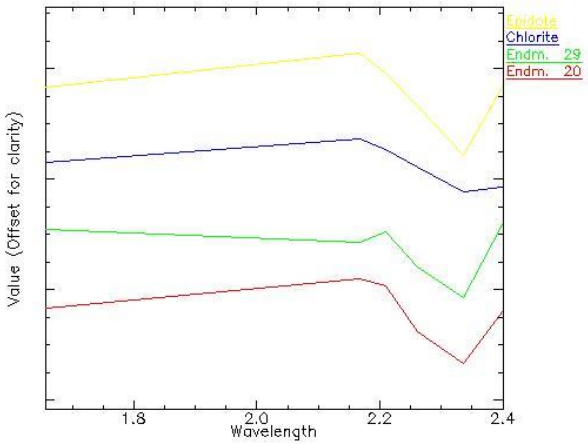

Fig. 20. Comparison of Library Spectral Profiles with Selected Endmembers for Chlorite and Epidote Minerals

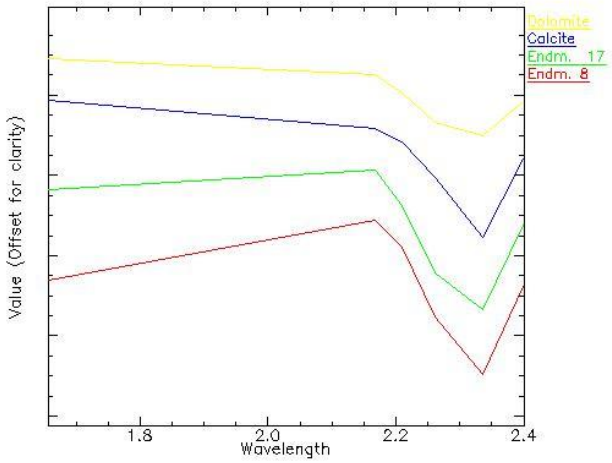

Fig. 21. Comparison of Library Spectral Profiles with Selected Endmembers for Dolomite and Calcite Minerals

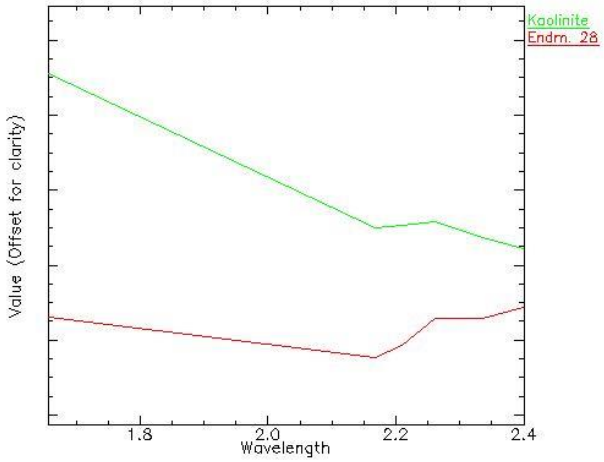

Fig. 22. Comparison of Library Spectral Profiles with Selected Endmembers for the Kaolinite Mineral

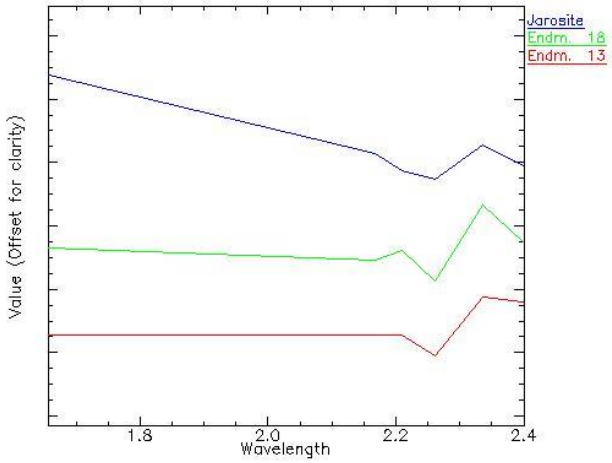

Fig. 23. Comparison of Library Spectral Profiles with Selected Endmembers for the Jarosite Mineral

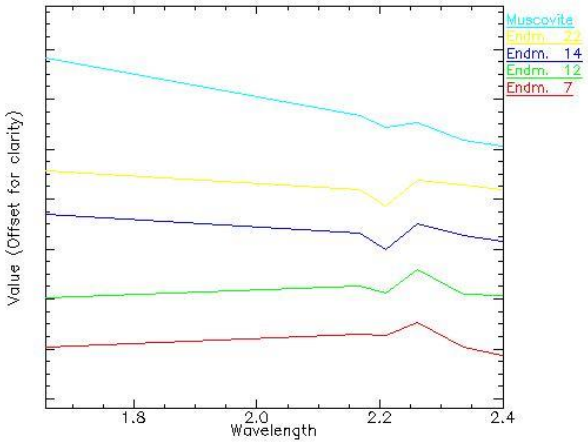

Fig. 24. Comparison of Library Spectral Profiles with Selected Endmembers for Muscovite and Sericite Minerals

3) Delineating Areas Containing Selected Endmembers

To delineate areas containing different materials, supervised classification methods were used after selecting appropriate endmembers. As previously mentioned, classification methods can be divided into two categories: Per-pixel and sub-pixel classifications. In this study, Per-pixel classification using the SAM method and sub-pixel classification using MTMF were employed.

a) Per-Pixel Classification

In Per-pixel classification, each pixel is compared with a reference spectrum and assumed to represent a single pure material. Hence, there is no mixing within the pixel, and only the degree of similarity to the reference spectrum is assessed. One such method is the Spectral Angle Mapper (SAM). SAM is a rapid classification method that assesses the similarity between image spectra and reference spectra to map geological units. This process involves calculating the spectral angle between the image spectra and reference spectra, producing outputs that indicate angular distances between zero and one, with smaller angles indicating greater similarity. Darker pixels in SAM images represent areas with smaller spectral angles, showing the highest similarity to the reference spectrum.

The SAM algorithm calculates similarity using the following equation:

$$\alpha = cos^{-1}\left[\frac{\sum_{i=1}^{nb} t_i r_i}{[\sum_{i=1}^{nb} t_i^2]^{1/2}[\sum_{i=1}^{nb} r_i^2]^{1/2}}\right] \quad (2)$$

Where n is the number of bands, t_i represents the test spectrum, and r_i represents the reference spectrum. This algorithm has been widely used by remote sensing scientists for lithological unit mapping. In SAM, the darkest points in the image are identified as the target areas (Mirsepahvand et al., 2022; Tangestani et al., 2008). The results of this method are presented in the Fig. 25 to Fig. 31.

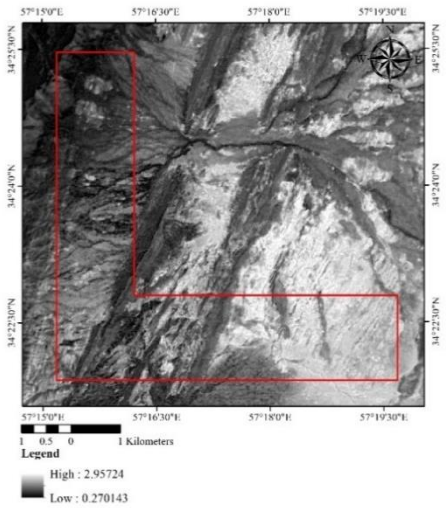

Fig. 25. Rule File for Endmember No. 8 Related to Calcite and Dolomite Minerals

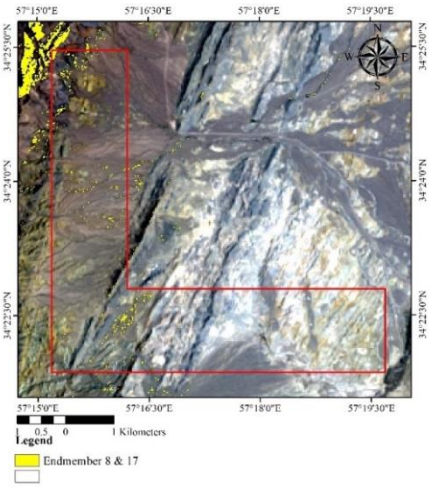

Fig. 26. SAM-Derived Segmented Regions for Endmembers No. 8 and 17

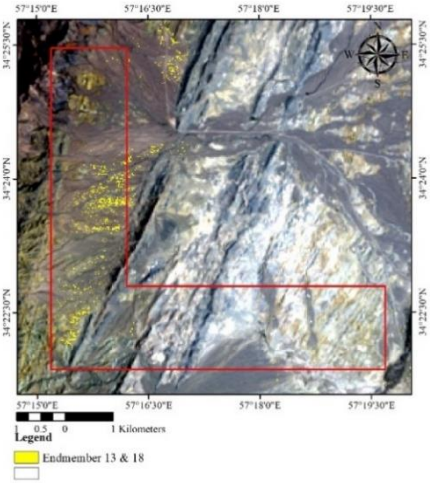

Fig. 27. SAM-Derived Segmented Regions for Endmembers No. 13 and 18

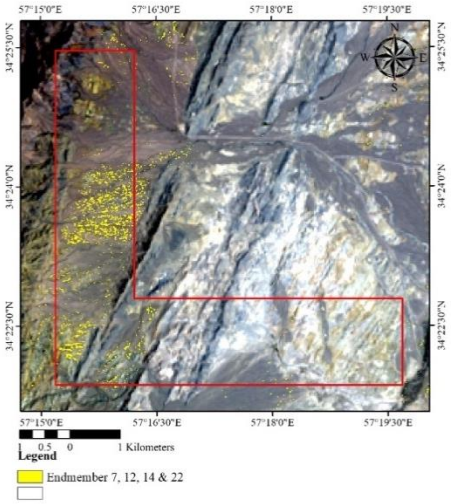

Fig. 28. SAM-Derived Segmented Regions for Endmembers No. 7, 12, 14, and 22

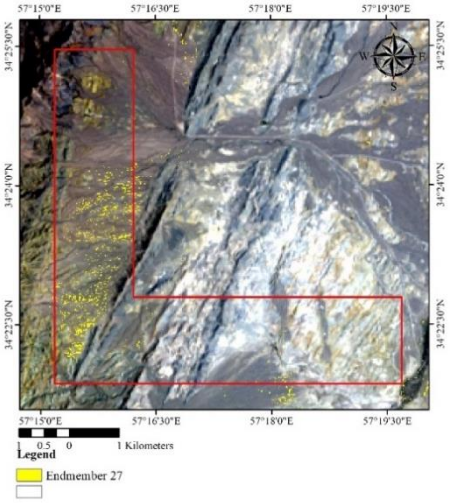

Fig. 29. SAM-Derived Segmented Regions for Endmember No. 27

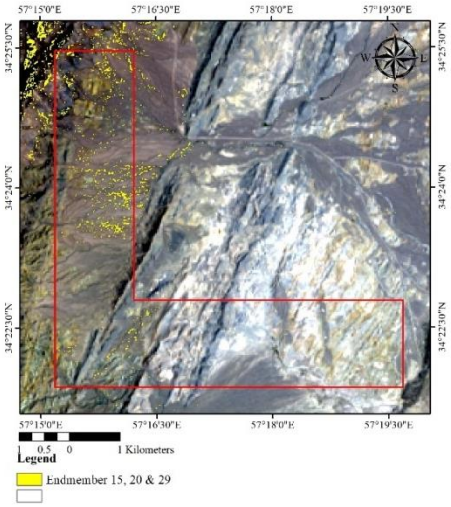

Fig. 30. SAM-Derived Segmented Regions for Endmembers No. 15, 20, and 29

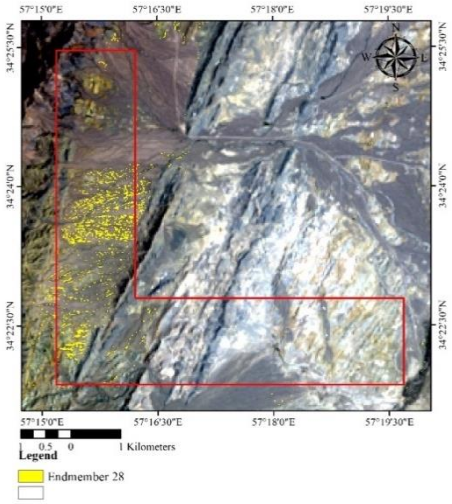

Fig. 31. SAM-Derived Segmented Regions for Endmember No. 28

b) Sub-Pixel Classification

Full-pixel classification assumes each pixel represents a single pure material, which is not always valid. The spatial resolution of sensors like ASTER (15m to 90m) often covers mixed materials within a pixel. Some surface materials inherently have mixed properties. In contrast to traditional classification where a pixel is assumed to be pure and assigned to a single material, sub-pixel classification allows a pixel to represent more than one material. The Mixture-Tuned Matched Filtering (MTMF) approach is one of the sub-pixel classification methods used to separate mixed materials within a pixel.

MTMF does not require knowledge of all the endmembers in the image, which is one of its key advantages. By introducing even a single spectrum, this method can filter and refine the pixels. MTMF results are displayed as two images: the matched filter (MF) image and the infeasibility image. By comparing the data in these two images in a two-dimensional space, pixels with high MF values and low infeasibility scores can be identified and evaluated for mapping (Hosseinjani et al., 2011; Modabberi et al., 2017; Tayebi et al., 2015). Fig. 32 and Fig. 33 show the MF and infeasibility images for endmember 8. The classified results of dividing MF by infeasibility for the end members are presented in Fig. 34 to Fig. 40.

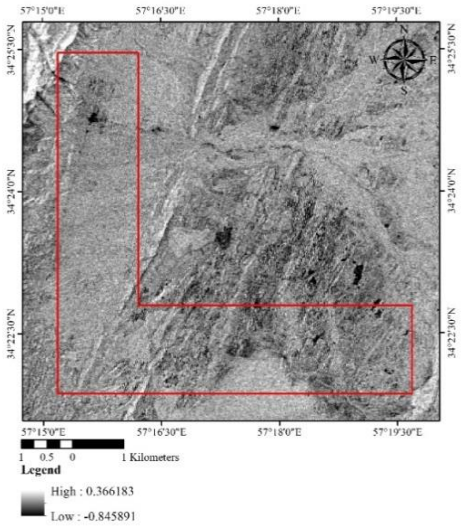

Fig. 32. Image Resulting from the Application of the Matched Filter for Endmember No. 8

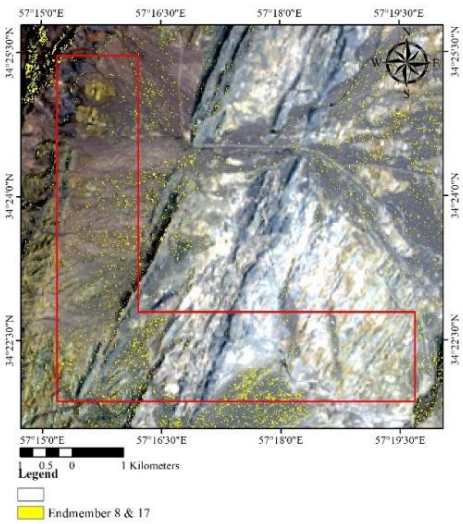

Fig. 35. MTMF-Derived Segmented Regions for Endmembers No. 8 and 17

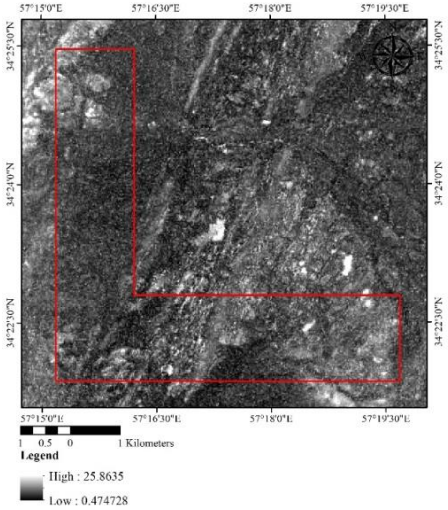

Fig. 33. Image Resulting from the infeasibility for Endmember No. 8

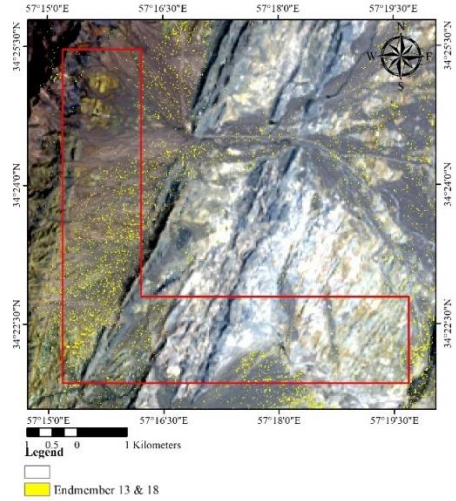

Fig. 36. MTMF-Derived Segmented Regions for Endmembers No. 13 and 18

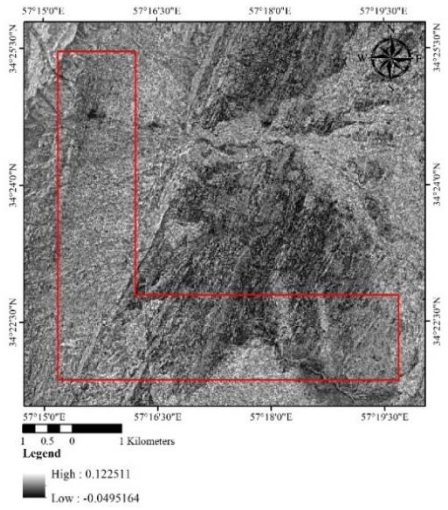

Fig. 34. Image Resulting from Dividing MF by Infeasibility for Endmember No. 8

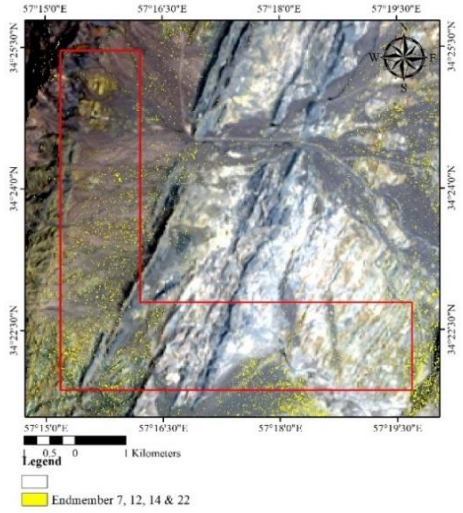

Fig. 37. MTMF-Derived Segmented Regions for Endmembers No. 7, 12, 14, and 22

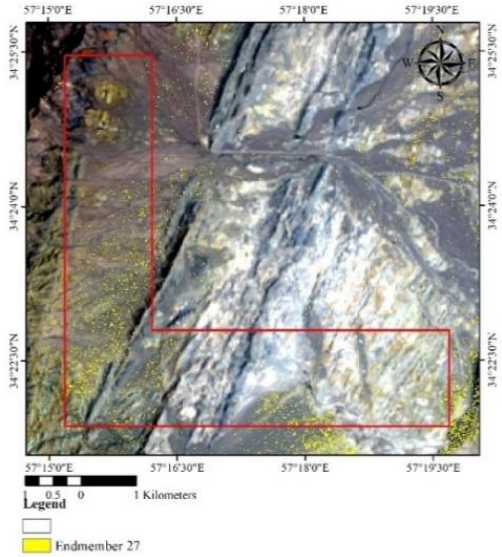

Fig. 38. MTMF-Derived Segmented Regions for Endmember No. 27

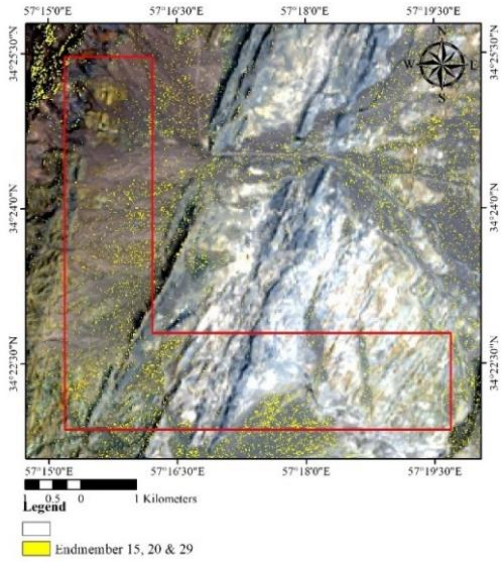

Fig. 39. MTMF-Derived Segmented Regions for Endmembers No. 15, 20, and 29

V. DISCUSSION

In this study, dolomitic, silicic, iron oxide, sericite, and argillic alterations were highlighted using false color composite and various band ratio methods from satellite images. Following this, two spectral analysis techniques were applied for more precise identification and differentiation of key minerals associated with these alterations: SAM (Spectral Angle Mapper) for full-pixel identification and MTMF (Mixture Tuned Matched Filtering) for sub-pixel identification.

In the SAM method, the spectral angle between image pixels and reference mineral spectra was calculated to map areas containing specific minerals. This method, due to its ability to detect pixels whose spectra closely resemble the reference spectra, offers high accuracy in mineral discrimination. Additionally, the MTMF method, based on a composite analysis and adaptive filtering approach, facilitated the detection of minerals at sub-pixel levels. This method is beneficial in regions where minerals exist in combination with other materials or in small quantities. The results from these analyses showed that the mineral maps produced using SAM and MTMF methods align closely with the outcomes from band ratio and false color composite techniques. This consistency between various methods increases confidence in the existence of alterations associated with mineralization in the studied area.

By analyzing satellite imagery and integrating the results, the northern and southern parts of the study area were identified as promising regions for further exploration. Significant alteration zones are observed in both sections. A large portion of the area is affected by iron oxide and dolomitic alterations, indicative of hydrothermal activities and associated alteration processes. Additionally, a limited area exhibited sericite alteration, which corresponds to the presence of minerals such as muscovite and sericite. Argillic and propylitic alterations were observed only in limited northern zones and the western boundary outside the study area. These alterations typically occur in hydrothermal systems and suggest potential areas of high mineralization prospects (Fig. 41).

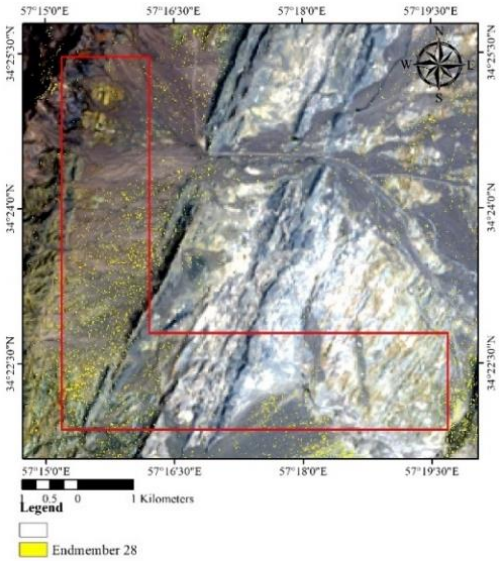

Fig. 40. MTMF-Derived Segmented Regions for Endmember No. 28

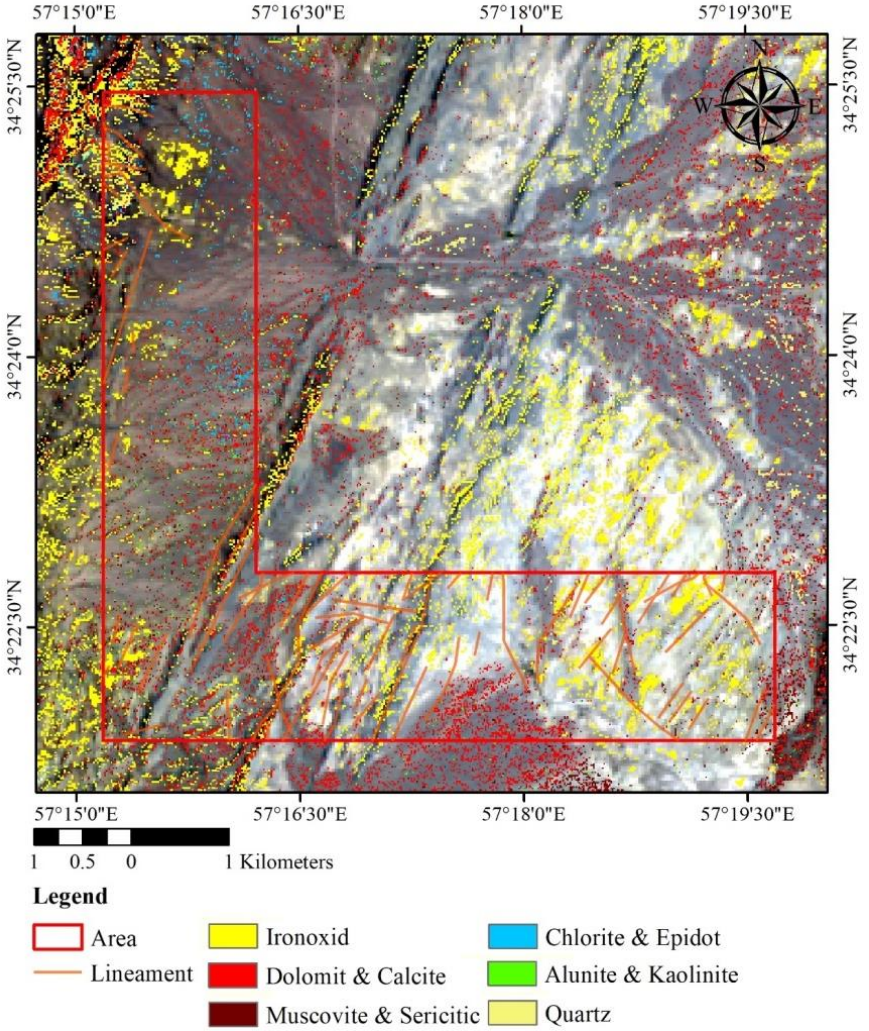

Fig. 41. Separated alteration regions of the study area

Hydrothermal systems are one of the primary mechanisms for mineral deposition, formed by complex processes of heat and material transfer within host rocks. One of the key indicators of hydrothermal activity is the presence of iron oxides such as hematite (Fe_2O_3) and goethite (FeO(OH)), which often result from chemical alterations and oxidation of hydrothermal fluids in the presence of oxygen. These oxides not only serve as by-products of hydrothermal processes but also act as important geochemical indicators for base metal mineralization, including copper (Cu) and iron (Fe), as well as precious metals like gold (Au) (Pirajno, 2008). Dolomitic alteration ($CaMg(CO_3)_2$) in hydrothermal environments is an indicator of hydrothermal fluids rich in magnesium. This type of alteration is usually associated with medium to high-temperature alteration processes, which form as hydrothermal fluids interact with carbonate rocks. Dolomite, due to its suitable crystalline structure and chemical stability, acts as an ideal host for the deposition of minerals like galena (PbS), sphalerite (ZnS), fluorite (CaF_2), and barite ($BaSO_4$). The presence of these minerals suggests the transfer of elements within hydrothermal systems and deposition within fractured and faulted environments through which the fluid flows (Leach et al., 2010). Additionally, the genetic link between hydrothermal alterations and geological structures, particularly lineaments and faults, indicates that these structures act as main channels for the transport of hydrothermal fluids. In this process, the pressure concentration and high temperatures along fault zones facilitates the deposition of base metals and sulfide minerals (such as pyrite, chalcopyrite ($CuFeS_2$), and sphalerite). This suggests the concentration of vein-type mineralization along these structures and highlights the importance of detailed structural analysis in evaluating the mineral potential of an area (Hedenquist et al., 1994).

Given the widespread dolomitic and iron oxide alterations, the area holds significant potential for lead and zinc mineralization. The dolomitic alteration, as a prominent feature in the region, points to hydrothermal activities with magnesium-rich chemical compositions that could create favorable conditions for the deposition of lead minerals like galena (PbS) and zinc minerals like

sphalerite (ZnS). This alteration typically occurs in medium to high-temperature hydrothermal systems, where dolomite acts as an ideal host, providing the right conditions for the accumulation and concentration of these metals. In addition to lead and zinc, the region has promising potential for iron mineralization due to the widespread presence of iron oxides like hematite and goethite. These oxides, as products of hydrothermal activities, could indicate alteration processes related to iron ore formation. Furthermore, hydrothermal activities associated with iron oxides and argillic and sericitic alterations increase the potential for gold in the region. In areas where hydrothermal alterations, especially sericitic and argillic, are present, there is also a likelihood of gold mineralization. Thus, the presence of a suite of base metals such as lead, zinc, iron, and gold, along with industrial minerals like fluorite and barite, indicates the high potential of the area for multiple types of mineralization.

VI. Conclusion

In this study, the application of spectral analysis methods SAM and MTMF allowed for accurate discrimination of key minerals, with results that closely matched other methods. The northern and southern parts of the area were identified as promising zones for further exploration, especially given the extensive alterations associated with hydrothermal activities. The strong relationship between alterations and geological structures, such as lineaments, suggests a high potential for mineralizing base metals like copper, iron, lead, and zinc, as well as precious metals like gold and industrial minerals like fluorite and barite. Future studies should focus more on these areas, particularly along lineaments, with detailed ground sampling and geochemical analyses to refine the results of this study and more precisely evaluate the mineral potential of the region.

REFERENCES

Aggarwal, S. (2004). Principles of remote sensing. Satellite remote sensing and GIS applications in agricultural meteorology, 23(2), 23-28.

Aghanabati, A., Ruttner, M., Nabavi, M., Hajian, J., & Alavi-Naini, M. (1994). Geological Sheet Map of Eshgh-Abad. Geological Survey of Iran.

Ahmadi, H., & Pekkan, E. (2021). Fault-based geological lineaments extraction using remote sensing and GIS—a review. Geosciences, 11(5), 183.

Amer, R., Kusky, T., & El Mezayen, A. (2012). Remote sensing detection of gold related alteration zones in Um Rus area, Central Eastern Desert of Egypt. Advances in Space Research, 49(1), 121-134.

Beiranvand Pour, A., & Hashim, M. (2014). ASTER, ALI and Hyperion sensors data for lithological mapping and ore minerals exploration. SpringerPlus, 3, 1-19.

Bernstein, L. S., Jin, X., Gregor, B., & Adler-Golden, S. M. (2012). Quick atmospheric correction code: algorithm description and recent upgrades. Optical engineering, 51(11), 111719-111719.

Boloki, M., & Poormirzaee, M. (2010). Using ASTER image processing for hydrothermal alteration and key alteration minerals mapping. Journal of Latest Trends on Engineering Mechanics, Structures, Engineering Geology, 1, 77-82.

Campbell, J. B., & Wynne, R. H. (2011). Introduction to remote sensing. Guilford press.

Chen, Q., Xia, J., Zhao, Z., Zhou, J., Zhu, R., Zhang, R., Zhao, X., Chao, J., Zhang, X., & Zhang, G. (2022). Interpretation of hydrothermal alteration and structural framework of the Huize Pb–Zn deposit, SW China, using Sentinel-2, ASTER, and Gaofen-5 satellite data: Implications for Pb–Zn exploration. Ore Geology Reviews, 150, 105154.

Dasgupta, S., & Mukherjee, S. (2019). Remote sensing in lineament identification: examples from western India. In Developments in Structural geology and Tectonics (Vol. 5, pp. 205-221). Elsevier.

Ding, H., Jing, L., Xi, M., Bai, S., Yao, C., & Li, L. (2023). Research on Scale Improvement of Geochemical Exploration Based on Remote Sensing Image Fusion. Remote Sensing, 15(8), 1993.

Esmaeilzadeh, N., Barak, S., Gani, N. D., Imamalipour, A., Abedi, M., & Pour, A. B. (2023). Alteration Zones Detection Using Image-Based and Spectrum-Based Image Processing Techniques to Aster Data: Sonajil Copper Deposit. IGARSS 2023-2023 IEEE International Geoscience and Remote Sensing Symposium,

Feizi, F., & Mansouri, E. (2012). Identification of alteration zones with using ASTER data in a part of Qom Province, Central Iran. Journal of Basic and Applied Scientific Research, 2(10), 10173-10184.

Gruninger, J. H., Ratkowski, A. J., & Hoke, M. L. (2004). The sequential maximum angle convex cone (SMACC) endmember model. Algorithms and technologies for multispectral, hyperspectral, and ultraspectral imagery X,

Hdeid, O. M., Morsli, Y., Raji, M., Baroudi, Z., Adjour, M., Nebagha, K. C., El Arby, Z., El Moktar, V. M., & Vall, I. B. (2024). Application of Remote Sensing and GIS in Mineral Alteration Mapping and Lineament Extraction Case of Oudiane Elkharoub (Requibat Shield, Northern of Mauritania). Open Journal of Geology, 14(9), 823-854.

Hedenquist, J. W., & Lowenstern, J. B. (1994). The role of magmas in the formation of hydrothermal ore deposits. Nature, 370(6490), 519-527.

Honarmand, M., Ranjbar, H., Shahriari, H., & Naseri, F. (2018). Evaluating the effect of using different reference spectra on SAM classification results: an implication for hydrothermal alteration mapping. Journal of Mining and Environment, 9(4), 981-997.

Hosseinjani, M., & Tangestani, M. H. (2011). Mapping alteration minerals using sub-pixel unmixing of ASTER data in the Sarduiyeh area, SE Kerman, Iran. International Journal of Digital Earth, 4(6), 487-504.

Hu, B., Xu, Y., Wan, B., Wu, X., & Yi, G. (2018). Hydrothermally altered mineral mapping using synthetic application of Sentinel-2A MSI, ASTER and Hyperion data in the Duolong area, Tibetan Plateau, China. Ore Geology Reviews, 101, 384-397.

Kabolizadeh, M., Rangzan, K., Mousavi, S. S., & Azhdari, E. (2022). Applying optimum fusion method to improve lithological mapping of sedimentary rocks using sentinel-2 and ASTER satellite images. Earth Science Informatics, 15(3), 1765-1778.

Kasmaeeyazdi, S., Braga, R., Tinti, F., & Mandanici, E. (2022). Mapping Bauxite Mining Residues Using Remote Sensing Techniques. Materials Proceedings, 5(1), 91.

Kayadibi, Ö. (2011). Evaluation of imaging spectroscopy and atmospheric correction of multispectral images (Aster and LandsaT 7 ETM+). Proceedings of 5th International Conference on Recent Advances in Space Technologies-RAST2011,

Kodama, S., Takeda, I., & Yamaguchi, Y. (2010). Mapping of Hydrothermally Altered Rocks using the Modified Spectral Angle Mapper (MSAM) Method and ASTER SWIR Data. International Journal of Geoinformatics, 6(1).

Leach, D. L., Taylor, R. D., Fey, D. L., Diehl, S. F., & Saltus, R. W. (2010). A deposit model for Mississippi Valley-type lead-zinc ores (2328-0328).

Marghany, M., & Hashim, M. (2010). Lineament mapping using multispectral remote sensing satellite data. International Journal of the Physical Sciences, 5(10), 1501-1507.

Mirsepahvand, F., Jafari, M., Afzal, P., & Arian, M. A. (2022). Identification of Alteration Zones using ASTER Data for Metallic Mineralization in Ahar region, NW Iran. Journal of Mining and Environment, 13(1), 309-324.

Modabberi, S., Ahmadi, A., & Tangestani, M. H. (2017). Sub-pixel mapping of alunite and jarosite using ASTER data; a case study from north of Semnan, north central Iran. Ore Geology Reviews, 80, 429-436.

Noori, L., Pour, A. B., Askari, G., Taghipour, N., Pradhan, B., Lee, C.-W., & Honarmand, M. (2019). Comparison of different algorithms to map hydrothermal alteration zones using ASTER remote sensing data for polymetallic vein-type ore exploration: Toroud–Chahshirin Magmatic Belt (TCMB), North Iran. Remote Sensing, 11(5), 495.

Okada, K., Segawa, K., & Hayashi, I. (1993). Removal of the vegetation effect from LANDSAT TM and GER imaging spectroradiometer data. ISPRS journal of photogrammetry and remote sensing, 48(6), 16-27.

Pirajno, F. (2008). Hydrothermal processes and mineral systems. Springer Science & Business Media.

Pour, A. B., Hashim, M., Park, Y., & Hong, J. K. (2018). Mapping alteration mineral zones and lithological units in Antarctic regions using spectral bands of ASTER remote sensing data. Geocarto International, 33(12), 1281-1306.

Pour, A. B., Hashim, M., & van Genderen, J. (2013). Detection of hydrothermal alteration zones in a tropical region using satellite remote sensing data: Bau goldfield, Sarawak, Malaysia. Ore Geology Reviews, 54, 181-196.

Sadek, M., Ramadan, T., El Leil, I. A., & Salem, S. (2006). Using remote sensing technique in lithological discrimination and detection of gold-bearing alteration zones at Wadi Defeit area, southeastern desert, Egypt. Remote sensing for environmental monitoring, GIS applications, and geology VI,

Scharcanski, J., & Venetsanopoulos, A. N. (1997). Edge detection of color images using directional operators. IEEE Transactions on Circuits and Systems for Video Technology, 7(2), 397-401.

Schmugge, T. J., Abrams, M. J., Kahle, A. B., Yamaguchi, Y., & Fujisada, H. (2003). Advanced spaceborne thermal emission and reflection radiometer (ASTER). Remote Sensing for Agriculture, Ecosystems, and Hydrology IV,

Schowengerdt, R. A. (2006). Remote sensing: models and methods for image processing. elsevier.

Spoto, F., Sy, O., Laberinti, P., Martimort, P., Fernandez, V., Colin, O., Hoersch, B., & Meygret, A. (2012). Overview of sentinel-2. 2012 IEEE international geoscience and remote sensing symposium,

Shebl, A., & Csámer, Á. (2021). Lithological, structural and hydrothermal alteration mapping utilizing remote sensing datasets: A case study around Um Salim area, Egypt. IOP Conference Series: Earth and Environmental Science.

Tangestani, M. H., Mazhari, N., Agar, B., & Moore, F. (2008). Evaluating Advanced Spaceborne Thermal Emission and Reflection Radiometer (ASTER) data for alteration zone enhancement in a semi-arid area, northern Shahr-e-Babak, SE Iran. International Journal of Remote Sensing, 29(10), 2833-2850.

Tayebi, M. H., & Tangestani, M. H. (2015). Sub pixel mapping of alteration minerals using SOM neural network model and hyperion data. Earth Science Informatics, 8, 279-291.

Tompolidi, A.-M., Sykioti, O., Koutroumbas, K., & Parcharidis, I. (2020). Spectral unmixing for mapping a hydrothermal field in a volcanic environment applied on ASTER, Landsat-8/OLI, and Sentinel-2 MSI Satellite Multispectral Data: The Nisyros (Greece) case study. Remote Sensing, 12(24), 4180.

Trahanias, P. E., Karakos, D., & Venetsanopoulos, A. N. (1996). Directional processing of color images: theory and experimental results. IEEE Transactions on Image Processing, 5(6), 868-880.

Van der Meer, F. D., Van der Werff, H. M., Van Ruitenbeek, F. J., Hecker, C. A., Bakker, W. H., Noomen, M. F., Van Der Meijde, M., Carranza, E. J. M., De Smeth, J. B., & Woldai, T. (2012). Multi-and hyperspectral geologic remote sensing: A review. International journal of applied Earth observation and geoinformation, 14(1), 112-128.

Yao, F., Xu, X., Yang, J., & Geng, X. (2021). A Remote-Sensing-Based Alteration Zonation Model of the Duolong Porphyry Copper Ore District, Tibet. Remote Sensing, 13(24), 5073.

Yousefi, S., Ranjbar, H., Alirezaei, S., & Dargahi, S. (2018). Application of mixture tuned matched filtering on ASTER data for hydrothermal alteration mapping related to porphyry cu deposits in Jabal-Barez Ranges, Kerman Copper Belt, Iran. Journal of Sciences, Islamic Republic of Iran, 29(3), 271-280.